Angle-resolved Auger study of 10-keV Ar^+-ion-induced Si *LMM* atomic lines

A. Bonanno, F. Xu, M. Camarca, R. Siciliano, and A. Oliva
Department of Physics, University of Calabria, I-87036 Rende, Cosenza, Italy
and Unità di Cosenza, Gruppo Nazionale di Struttura della Materia (GNSM) del Consiglio Nazionale delle Richerche e Centro Interuniversitario di Struttura della Materia (CISM) del Ministero della Pubblica Istruzione, I-87036 Rende, Cosenza, Italy
(Received 20 November 1989)

We present a detailed, angle-resolved Si *L*-shell Auger study by bombarding a single-crystalline Si sample with 10-keV Ar^+ ions. We have observed a new atomic line at kinetic energy of ~99 eV which is tentatively assigned to an Auger transition involving two 2*p* holes in Si^+. The existence of two atomic peaks at 61.36 and 91.1 eV has also been clearly confirmed. Our Auger spectra show well-split Doppler peaks for the principal Si^0 and Si^+ atomic lines and a strong dependence of the shift amplitude on both incidence and detection angles. Successful computer fitting of the angular dependence of Doppler shift has been achieved by using a simple binary-collision model with the Molière approximation to the Thomas-Fermi screening potential. These results suggest that the first violent Ar-Si asymmetric collisions contribute remarkably to the Si 2*p*-vacancy creation process and are responsible for the ejection of energetic $Si^{(*)}$ particles which is highly directional. The critical minimum Ar-Si approach distance for Si 2*p*-hole excitation is 0.355 Å, in very good agreement with the value predicted by molecular-orbital theory.

I. INTRODUCTION

Studies of phenomena related to interactions between heavy ions and solid surfaces have attracted close attention in the past years for both fundamental reasons and practical applications in surface analysis.[1] These studies include sputtering of target particles (neutrals and/or ions), emission of photons, and secondary electrons.[2–5] Besides the typical yield measurements, some energy spectra and spatial distribution results of ejected particles have also become available recently in literature, providing a great deal of basic information about the physical mechanisms which govern these phenomena.[6–10] Target-species Auger-electron spectra excited by ion impact have been shown to be substantially different from those induced by conventional electron or photon excitation.[4,11–14] Many narrow atomiclike Auger lines superimposed on a broader feature have been observed for several light elements such as Mg, Al, and Si. The interpretation of these spectroscopic features was at one time a subject of controversy,[12,14–19] but now it is generally agreed that the atomiclike peaks are due to deexcitation of sputtered particles decaying in the free space outside the sample.[9,20] Because of the movement of the parent excited species relative to the analyzer, Doppler shifts in measured kinetic energies of emitted Auger electrons are expected.[21] In a previous angle-resolved study we reported clear evidence for the existence of well-shifted Doppler peaks for Si Auger lines under 10-keV Ar^+-ion bombardment.[9]

The observation of large Doppler shifts has a profound significance in studies of ion-solid interactions. These shifts provide important information about the spatial and energetic distributions of the excited atoms and/or ions, information that is not usually available from conventional secondary-ion mass spectroscopy (SIMS) studies. On this subject, recently we have reported some preliminary results and qualitative discussions regarding the distribution of ejected excited Si species under Ar^+-ion bombardment.[22]

This paper is a continuation of our studies on the Doppler effect concerning target atomic peaks. Ar-Si system has again been chosen because of the large cross section for Si *L*-shell excitation. The main purposes are: (i) to provide a detailed interpretation of the observed Si Auger spectroscopic features; (ii) to investigate the angular dependence of the Doppler shift of the principal Si^0 and Si^+ Auger lines; (iii) to discuss the Si 2*p*-vacancy creation mechanism(s); and (iv) to establish an energy and spatial distribution pattern for the sputtered fast moving $Si^{(*)}$ particles.

II. EXPERIMENT

Experiments were conducted in a ultrahigh-vacuum chamber equipped with a differentially pumped ion gun designed for sputtering studies with an acceleration energy ranging from 2 to 15 keV, an electron gun for conventional Auger studies, a mass spectrometer, and a hemispherical charge energy analyzer mounted on a rotatable goniometer for angle-resolved studies. The minimum angle between this analyzer and the ion beam allowed in our experimental layout was 25° and the analyzer acceptance angle was 2°. The chamber base pressure was 3×10^{-10} Torr and it rose to 6×10^{-9} Torr during ion-beam operation.

A single-crystalline Si wafer was mounted on a dedicated sample manipulator placed in the center of the chamber. Variation of ion or electron incidence angle was achieved by sample rotation and the analyzer was

placed in a specular reflection plane. The sample surface and energy analyzer were carefully aligned to assure rotations around the same axis which coincides with the focuses of ion or electron beam and that of the analyzer.

Data acquisition was facilitated by an on-line personal computer. For each spectrum 4096 data points were taken which correspond to a separation of 0.0125 eV between two consecutive channels in our scanning range (60–110 eV). Accumulation of more than 30 scans for each spectrum assured a good signal-to-noise ratio. The analyzer pass energy was set at 100 eV with an absolute energy resolution better than 1 eV, but the accuracy in determining peak separation was 0.15–0.2 eV. All spectra were taken in a pulse-counting mode (counting rate 10^4–10^5 sec^{-1}).

III. RESULTS AND DISCUSSIONS

A. Atomiclike Si Auger lines

In Figs. 1–3 we present some typical Si Auger spectra taken with 10-keV Ar^+-ion bombardment for various incidence and detection angles. The experimental geometry is sketched in Fig. 4. The ion-induced Si Auger spectrum consists of several narrow lines superimposed on a broad feature whose intensity decreases approximately according to a cosine law as the detection angle increases, similarly to the behavior of the conventional electron-induced Auger signals. This underlying continuum is commonly assigned to the *LVV* Auger transition occurring inside the Si matrix.[7,12,14] The intensities of the atomiclike peaks vary slightly going from normal to grazing emission angle, as observed previously by Yamauchi *et al.*,[23] and can be attributed to the possible surface roughness caused by bombardment.

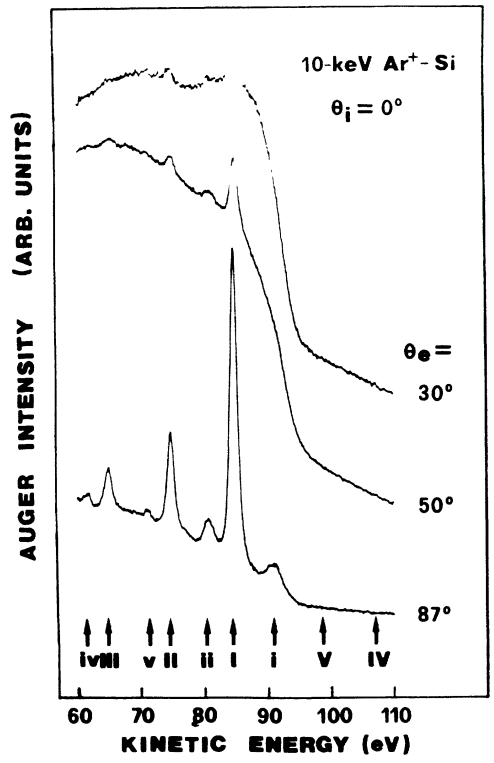

FIG. 1. Normalized Si Auger spectra taken with 10-keV Ar^+-ion bombardment for normal incidence and three different detection angles. The experimental geometry is schematically shown in Fig. 4. It can be seen that the broader bulk *LVV* feature decreases rapidly with increasing detection angle, as expected from an electron effective escape-depth consideration.

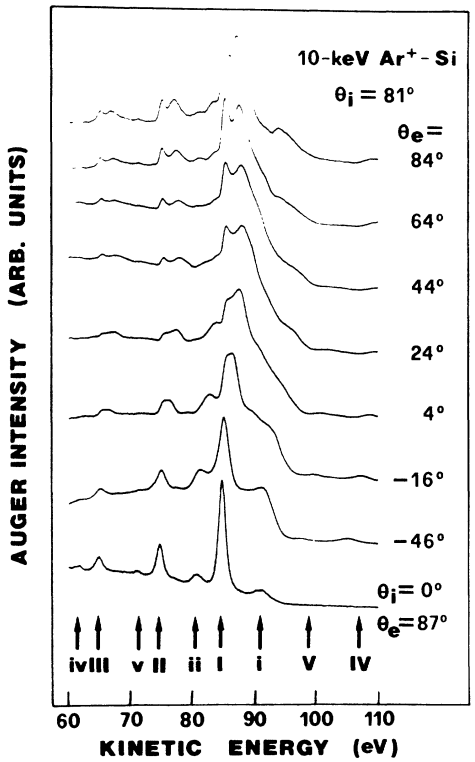

FIG. 2. Si Auger spectra taken with 10-keV Ar^+-ion excitation for a fixed incidence angle of $\theta_i = 81°$ and various electron detection angles. In the bottom a spectrum of $\theta_i = 0°$ and $\theta_e = 87°$ is reproduced from Fig. 1 for comparison. The peaks on the high-energy side of the main Auger transition lines are due to Doppler shifts caused by the fast movement of their parent $Si^{(*)}$ particles relative to the analyzer.

The Si *L*-shell core excitation mechanism for Ar^+-ion bombardment has been generally described within the framework of electron promotion via molecular orbital curve crossing developed by Fano and Lichten[24] and extended by Barat and Lichten.[25] The assignment of each of the atomic Auger features has been discussed in detail previously by Thomas *et al.*[14,26] Following their suggestions, we have labeled the sharp atomic peaks in our figures and listed the respective energy positions in Table I. Since the absolute measured kinetic energies depend on the resolution and on the work function of the spectrometer, we present also the experimental energy difference of various peaks with respect to the principal atomic line (I) and compare them with the available results in literature. It should be mentioned that comparison between the observed and predicted absolute kinetic energies can be made only in a relative sense because of

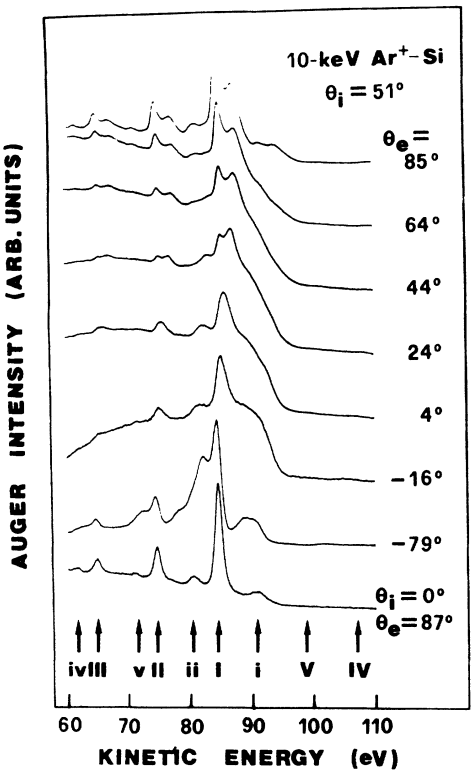

FIG. 3. Si Auger spectra induced by 10-keV Ar^+-ion impact for $\theta_i = 51°$ and various detection angles. Similar to those shown in Fig. 2 for $\theta_i = 81°$, the Doppler shifts again exhibit a strong dependence on θ_e. Note that for $\theta_e = -79°$ (the analyzer and the ion beam on the same side of the surface normal), the shifts are negative, indicating the forward target atom ejection.

the systematic uncertainty of a few eV in the latter values.[14,26]

It is very interesting to note the presence of a small peak (labeled iv in Figs. 1–3) situated at $E_{kin} = 61.36 \pm 0.10$ eV. This peak has been firstly observed by Saiki and Tonaka[27] (labeled P_2' in Fig. 1 of Ref. 27) but these authors did not provide any detailed information regarding its energy position and its physical nature. The narrow linewidth and its intensity dependence on detection angle suggest that it should also be ascribed to an Auger transition from sputtered Si particles decaying outside the sample. In a scheme proposed by Thomas *et al.*[26] this peak could have the lowest kinetic energy in the series of Si^+ Auger decays. In particular, we propose that it originates from the $2p^5 3s^2 3p^2 \rightarrow 2p^6 3p^2(^1P)$ transition in Si^+ ions. The fairly good agreement between our experimental finding of the energy separation, -13.23 ± 0.2 eV, between this peak and that of the main Si^+ line (peak II) and the theoretical value of -12.47 eV gives further confidence to our assignment. The absence of this feature in most previous studies could be attributed partially to the poorer energy resolution and/or the poorer statistics and partially to the different ion incidence energies, and thus to the different excitation cross sections.

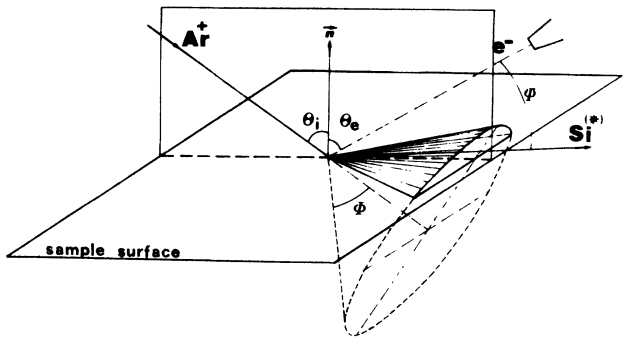

FIG. 4. Sketch of the experimental geometry and kinematics of the sputtered fast-moving $Si^{(*)}$ atoms (ions) and a binary Ar-Si collision model. Incidence ion beam, electron detector, and sample surface normal are in the same plane. The sputtered Si particles are distributed with a cone-type symmetry around the ion incidence direction. Φ is a generic scattering angle for such cones and Ψ is the angle between the analyzer and a generic ejection direction.

It has been observed by many research groups that the high-energy edge in the electron-induced spectra does not coincide exactly with that in the ion-induced spectra.[7,12,14] Thomas *et al.*[14,26] proposed the presence of an atomiclike peak (labeled i in Fig. 1) and suggested that it is due to the transition of $2p^5 3s^2 3p^3 \rightarrow 2p^6 3s^2 3p(^2P)$ in Si^0. De Ferraris *et al.*[28] by using grazing incidence have confirmed its atomic origin. Saiki and Tanaka,[7] on the base of the apparently similar angular dependence of its intensity to the peak excited by electrons, instead, favored the bulk nature of this Auger feature. In Fig. 5

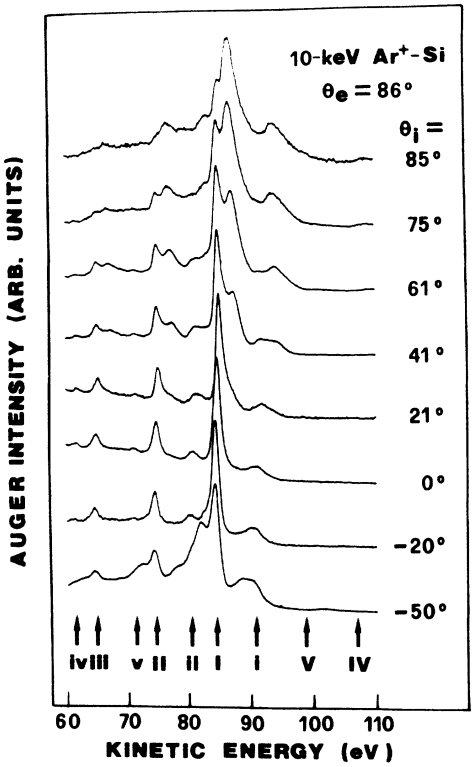

FIG. 5. 10-keV Ar^+-induced Si Auger spectra taken at a fixed very grazing angle $\theta_e = 86°$ for different incidence angles. These experimental conditions minimize the contributions from the Si bulk and emphasize the line-shape changes in peak i and peak V. Note that the Doppler shifts for the main transition lines strongly depend on the ion impinging direction.

TABLE I. Energies of atomiclike Si Auger lines.

Peak label	Species	Transition[b]	Predicted kinetic energy (eV)[b]	Observed kinetic energy (eV)	Observed relative energy (eV)[a] This study	Thomas[b]	Tanaka[c]	Wittmaack[d]
	Si^0	$2p^5 3s^2 3p^3$						
i		$2p^6 3s^2 3p(^2P)$	90.15	91.10	6.48±0.20	7.0	7.4	
		$2p^6 3s 3p^2(^4P)$	84.70					
I		$2p^6 3s 3p^2(^2D)$	83.30	84.62	0.00	0.0	0.0	0.0
ii		$2p^6 3s 3p^2(^2S)$	80.65	80.48	−3.78±0.20	−3.0	−4.1	
		$2p^6 3s 3p^2(^2P)$	79.71					
iii		$2p^6 3p^3(^4S)$	74.75			−8.0		
	Si^+	$2p^5 3s^2 3p^2$						
ii		$2p^6 3s^2(^1S)$	82.01	80.48	−3.78±0.20	−3.5	−4.1	
II		$2p^6 3s 3p(^3P)$	75.47	74.59	−10.03±0.15	−10.0	−10	−9.5
v		$2p^6 3s 3p(^1P)$	71.74	71.04	−13.58±0.15		−13.9	
		$2p^6 3p^2(^1D)$	66.90					
III		$2p^6 3p^2(^3P)$	65.34	64.78	−19.84±0.15	−20.0	−20	−19.5
iv		$2p^6 3p^2(^1P)$	63.00	61.36	−23.26±0.20			
	Si^+	$2p^4 3s^2 3p^3$						
IV		$2p^5 3s 3p^2$	103.7	107.0	22.4±0.3	21.0		21.5
V		$2p^5 3s 3p^2$		99.0	14.4±0.3			

[a]Reference to that of peak I.
[b]Reference 14.
[c]Reference 7.
[d]Reference 12.

we show several spectra taken at a very grazing detection angle $\theta_e = 86°$ for different incidence angles. These experimental conditions minimize the contribution from the Si bulk and emphasize the line shape changes in the peak i. The narrow linewidth and especially the observed Doppler shifts unambiguously reveal the atomic nature of this feature, providing conclusive support to the earlier interpretation of Thomas *et al.*

The Auger transition $L^{2*}MM$ in Si^+ with double L-shell vacancies, labeled as peak IV ($E_{kin} \sim 107$ eV), was observed in our experiments only for an ion incidence angle different from the surface normal (Figs. 2, 3, and 5), in agreement with the general contention that this peak is produced by projectile-target asymmetric collisions.[14,29,30] In fact, the kinematics of inelastic binary collision prohibits ejection of target atoms for scattering angles greater than 90° from the incident direction. The intensity of this doubly excited peak is generally very low in comparison with those of other Si Auger features, except for the case of high-energy Ar^+-ion bombardment (190 keV) reported by Thomas and co-workers.[14] A clear correlation of its peak intensity with the Ar L-shell Auger yield led Wittmaack to conclude that both Si and Ar could be excited in the same collision event.[29] The results shown in Figs. 2 and 5 clearly demonstrate that the efficiency of the creation of two $2p$ holes in the lighter collision partner (Si) is not so small as previously thought, not even in the relatively low incidence energy range as in the present study. This peak is commonly assigned to the transition of $2p^4 3s^2 3p^3 \rightarrow 2p^5 3s 3p^2$ in Si^+, however, other different initial states (doubly ionized or neutrally excited) and/or different final states are also possible.[14]

It is very interesting to note the presence of a new small peak which is situated in the kinetic energy range of 98–101 eV in Fig. 2 (labeled V) and lies on the tail of the peak i and the bulk LVV feature. This peak has never been observed before and could be clearly revealed only in some critical experimental conditions. In the absence of a detailed energy calculation, we tentatively suggest that it probably involves the same transition in doubly excited Si^+ as for the peak IV but with different initial and/or final spin-orbit configurations.

The Auger decays of these doubly excited states occur undoubtedly outside the sample, as can be readily inferred from their line shape and linewidths. As mentioned above, such excitations are caused by direct Ar-Si binary collisions, thus the energy transferred to the recoil Si particle could be quite large. On the other side, the lifetime of a doubly excited state is considerably shorter than that of a single L hole, therefore only those Si ions with quite high kinetic energies could escape from the surface and decay in the vacuum well beyond the effective range of the surface potential. Consequently, our experimental spectra show only Doppler shifted peaks without the usual unshifted components as for other Si Auger lines, and the absolute kinetic energies of these electrons in the rest frame are quite difficult to determine. (See Sec. III B for a detailed discussion on the Doppler effects.) An estimate from our results would suggest that they are centered at around $E_{kin} = 99$ and 107 eV, respectively.

B. Doppler shifts in Si atomic Auger lines

In Fig. 2 are shown a series of Si Auger spectra taken with 10-keV Ar^+ excitation for a fixed incidence angle $\theta_i = 81°$ as a function of electron detection angle θ_e. All the spectra have been normalized to the same height to emphasize the changes in line shape. A spectrum for $\theta_i = 0°$ and $\theta_e = 87°$ is reproduced in the bottom from Fig. 1 as a reference. It can be clearly noted that close to the narrow atomic Auger lines which have nearly invariant kinetic energies there are also new features on the high kinetic-energy side. The separation between the shifted peak and the main line varies considerably as the detection angle is changed. For the most intense peak (I), for $-46° \leq \theta_e \leq 29°$, the new component shifts continuously toward high kinetic energy, converting the asymmetric tail of the main Auger line to a well-developed satellite. The highest kinetic energy of 87.83 eV ($\Delta E = 3.21 \pm 0.15$ eV) for the spectral maximum is reached at $\theta_e = 29°$. A further increase in θ_e causes a reduction in the energy split. The peak position of this shifted Auger feature as a function of detection angle is plotted in the lower panel of Fig. 6. We point out that the presence of a varying bulk feature which underlies these atomic peaks, in principle, may introduce an artificial shift in determining their absolute kinetic energies; however, background subtraction does not seem to modify the peak positions of the main Auger doublet I sensitively, at least within our experimental uncertainty. The satellite linewidth, about 2–3 times of that of the main peak, varies gradually as the detection angle is varied. Very similar behaviors are observed for the satellite of peak II (due to an Auger transition in Si^+), and the shift amplitude versus the detection angle is summarized in the lower panel of Fig. 7.

As we discussed in detail in a previous paper,[9] the satellites at high kinetic-energy sides have the same physical origins of the main peaks from which they split off, but the measured kinetic energies of these Auger electrons are Doppler shifted due to the fast movement, relative to the analyzer, of their parent Si particles. The experimental findings that the satellites have relatively narrow linewidths (2–3 eV) and assume maximum values for Doppler shift strongly suggest that the ejection of the majority of fast-moving target particles occurs along certain preferential direction(s) and that the speed of such species is well defined with a small spread. In fact, a nearly isotropic spatial distribution or a nearly uniform velocity distribution would result only in a large broadening of the main peak but could not give rise to a well separated satellite.

In Fig. 3 are shown some Si Auger electron spectra taken at different detection angles for an ion incidence angle of $\theta_i = 51°$. These spectra shown both similarities and differences with respect to those presented in Fig. 2 for $\theta_i = 81°$. As can be seen, the Doppler shift again depends on the electron detection angle (see the upper panels of Figs. 6 and 7), confirming our earlier argument that the Auger electrons are emitted from the energetic excited Si atoms and ions moving along some preferential direction(s). Moreover, when the analyzer is placed at

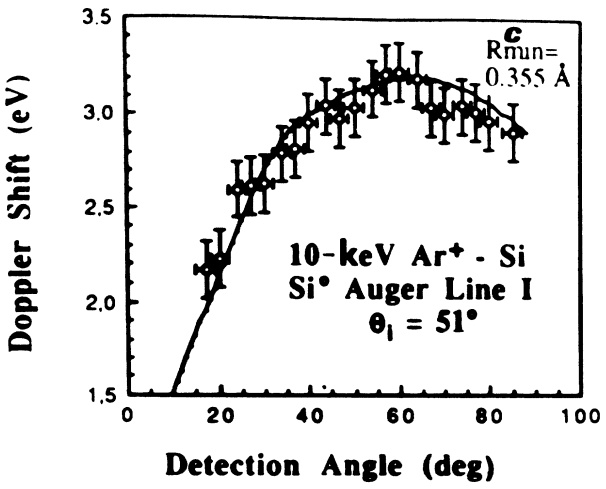

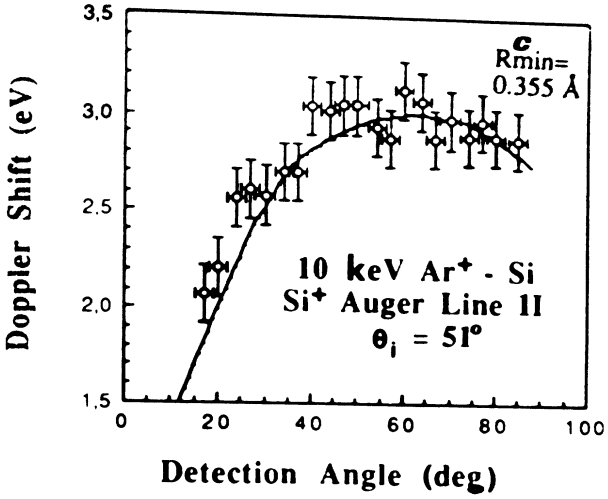

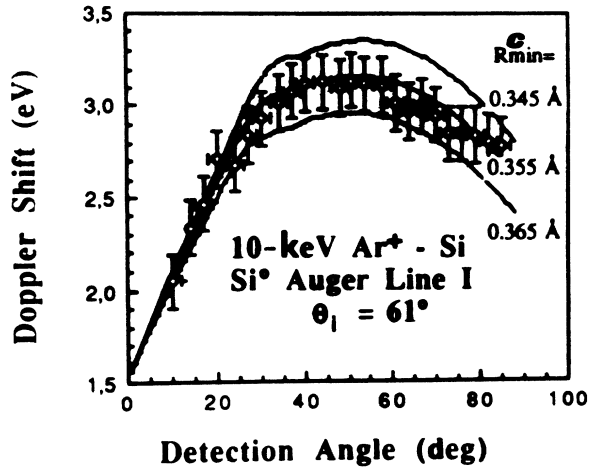

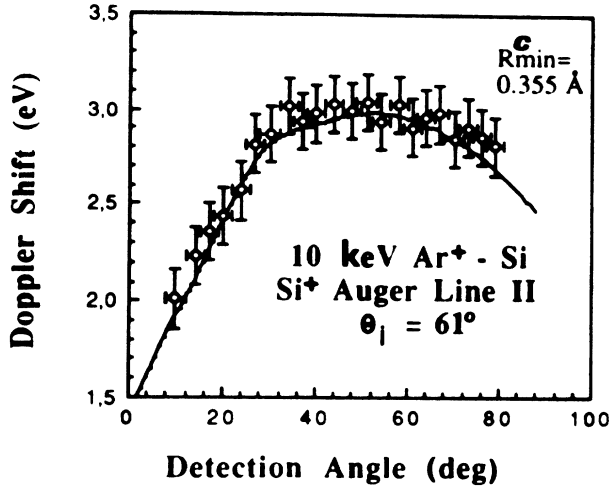

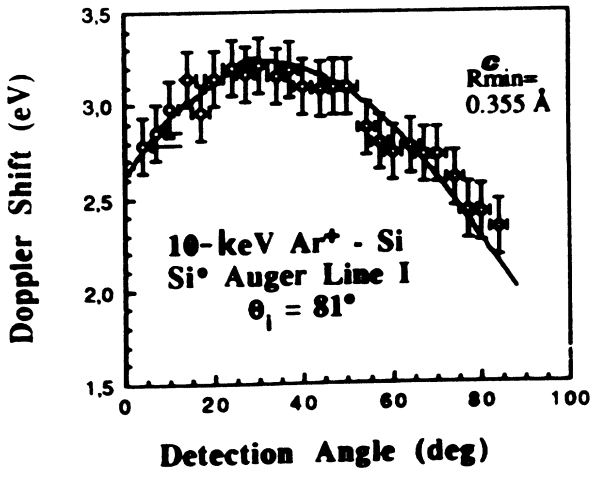

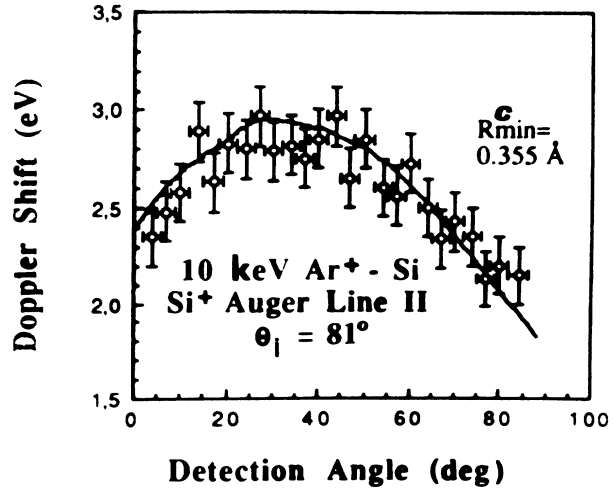

FIG. 6. Doppler shift for the most intense Si^0 Auger transition, labeled I in Figs. 2 and 3, as a function of electron detection angle for different ion incidence angles. The continuous curves are the fittings with a simple binary Ar-Si collision model using a critical minimum approach distance for excitation of $R^c_{min}=0.355$ Å.

FIG. 7. Doppler shift for the Auger peak II of Si^+ vs the detection angle for a few ion incidence angles. The continuous curves are the fitting results using a binary Ar-Si asymmetric collision model. The critical minimum approach distance is $R^c_{min}=0.355$ Å, the same as in the Si^0 case.

$\theta_e = -79°$ (analyzer and ion beam on the same side of the surface normal), well-resolved negatively shifted components appear at the low kinetic-energy side for all the principal Auger peaks, indicating that their parent particles move away from the detector. We also note that the detection angle corresponding to the maximum split shows a strong dependence on the ion incidence angle.

To get further insight into the mechanism of the ejection of excited fast-moving Si atoms, we fixed the electron detection angle ($\theta_e = 86°$) and varied the ion-beam incidence angle (from $\theta_i = -50°$ to $\theta_i = 85°$). Several representative spectra are shown in Fig. 5. They are very similar to those taken at fixed incidence angle and different detection angles (Figs. 2 and 3), showing a gradual variation of the Doppler component at θ_i is changed.

The large Doppler shift and its strong dependence on both incidence and detection angles observed in our experiments lead us to conclude that the fast-moving excited Si particles are produced by the primary violent Ar-Si asymmetric collisions but not by Si-Si interactions in the successive collision cascade. Indeed, in most of the cascade events the energy transfer is relatively small, and there does not exist a clear correlation between the kinetic energy and the ejection direction of outgoing excited atoms.

The absence of a well-separated Doppler peak for all detection angles in the case of normal ion incidence (Fig. 1 and Ref. 7) provides further support to our conclusion that the sputtered fast moving $Si^{(*)}$ and $Si^{+(*)}$ particles are produced by the primary violent Ar-Si asymmetric collisions. In fact, in a binary collision the backward scattering of the target atom is not allowed by the kinematics.

As far as the unshifted Auger lines are concerned, they can be produced in cascade events either by Si-Si symmetric collisions or by Ar-Si asymmetric collisions. Because the impinging Si or Ar particle should have a minimum kinetic energy to be able to penetrate into the rest Si atom in order to excite a $2p$ electron (either in the projectile or the target Si atom),[25] and because in such an inelastic collision the transferred kinetic energy may also be quite large, we expect that the ejected excited Si particles could have a non-negligible average kinetic energy to induce a slight Doppler broadening in the unshifted components in measured Auger spectra. Further, consideration based on the symmetry of experimental geometry would also suggest that for normal ion incidence, the spectrum taken at a very grazing detection angle should have a nearly symmetric broadening on both low- and high-energy sides, as is indeed observed in our experiments.

It has been argued in many previous studies[16,31] that the symmetric Si-Si collisions are the main mechanism for the Si L-shell hole creation. Wittmaack[12] observed an enhanced Auger yield for Ar^+ incidence energy greater than 4 keV, and suggested that the asymmetric Ar-Si collisions contribute remarkably to the Si inner-shell excitation process. The Si Auger yield measurements in gas-phase Si^+-Ar collisions reported by Schneider *et al.*[32] provided direct evidence that asymmetric collisions can produce Si L-shell excitation; however, it should be mentioned that their primary energies of the impinging Si^+ ions were higher than 35 keV.

Pepper and Aron[33] observed the Doppler-shifted target Al Auger lines for several particular incidence and emission angles for the system Ne^+-Al. They also found a strong angular dependence of the line shape of the shifted Al peak, and speculated that the energy distribution of the fast ejected $Al^{(*)}$ flux is relatively narrow. In a recent study of Monte Carlo simulation of the Ar^+-Al system in comparison with experimental Auger yields, Grizzi and Baragiola[34] found that for low incidence ion energies (≤ 4 keV) the symmetric target-target collisions dominate in the Al L-shell excitation process, while for higher energies the projectile-target asymmetric collisions become increasingly important. These findings have been confirmed independently by Hou *et al.*[35]

C. Binary collision model for the spatial and energetic distribution of sputtered fast $Si^{(*)}$ particles

As we have discussed in the previous section, the ejection of fast moving $Si^{(*)}$ particles is produced by the first violent Ar-Si binary collisions. The strong dependence of the Doppler shift on both incidence and detection angles also suggests that the ejection of these energetic sputtered species is highly directional. It is the aim of this section to use a simple binary collision model to account for the observed angular dependence of the Doppler shifts for the principal Si Auger lines, thus to establish a spatial and energetic distribution pattern for these ejected Si atoms and ions.

In an angle-resolved Ne Auger line-shape study for the Ne^+-Al system, Pepper[36] has developed a binary collision model using the Molière approximation to the Thomas-Fermi screened Coulomb interaction potential with a Firsov screening length to trace the neon trajectory. The critical closest Ne-Al approach distance for the creation of an Al $2p$ hole was chosen to be the sum of the $2p$- shell radii of Al and Ne. The calculated $2p$ Auger spectra resembled quite well the experimental results. Detailed descriptions can be found in Ref. 36.

In our Si L-shell Auger Doppler-shift studies for Ar^+-Si collisions this binary collision model has been used. Differently from Pepper's computer-fitting procedure, we have included the inelastic energy loss during collisions in the kinematical calculations,[37] and we have fixed the kinetic energy of the Si $2p$ Auger electrons in the rest frame as to be equal to that experimentally measured from the spectrum taken at $\theta_i = 0°$ and $\theta_e = 87°$, where no shifts were observed, and we have tried the critical minimum Ar-Si approach distance for excitation to yield the best agreement between the experimental Doppler shifts and calculated values.

It should be mentioned that in our computer fittings the effect of surface potential has been neglected. This is justified by the smallness of such a potential (7.8 eV) (Ref. 38) in comparison with the kinetic energy of incident Ar^+ ions (10 keV) and that of sputtered $Si^{(*)}$ particles

(≥ 1.2 keV; see the following discussions).

In Fig. 8 we show the calculated differential cross section and transferred kinetic energy for $Si^{(*)}$ recoils for the inelastic scattering events as a function of scattering angle in the laboratory system. The vertical line in the figure represents the threshold corresponding to a closest approach distance of 0.355 Å. In calculating these spatial and energetic distribution patterns of sputtered $Si^{(*)}$ particles, an energy loss of $Q=100$ eV for an L-shell electron excitation[13] has been included in kinematical transformation from the center-of-mass system to the laboratory system.

To determine the critical minimum Ar-Si approach distance R^c_{min} for exciting $Si^{(*)}$ L-shell Auger electrons, we have fitted the experimental Doppler shifts using a least-squares fitting procedure for each set of measurements for a given incidence angle θ_i. In doing so, the Si $2p$ electron excitation probability is assumed to be equal to unity once the minimum approach distance reaches or becomes less than a critical value R^c_{min}, and to be equal to zero otherwise. In Fig. 6 we show our results (continuous curves) for the Doppler shift relative to the main $Si^{(*)}$ Auger line (peak I) as a function of detection angle for various Ar^+-ion incidence angles using an Auger energy of $E_{Auger}-\Phi=84.62$ eV, determined from the spectrum for $\theta_i=0°$ and $\theta_e=87°$, where $\Phi=4.5$ eV is the spectrometer work function. We found that, in contrast to what was claimed by Pepper in his modeling of the Ne^+-Al case, the fitting quality depends sensitively on the value of R^c_{min}, as clearly demonstrated by the continuous curves shown in the middle panel of Fig. 6 for $\theta_i=61°$. In fact, the R^c_{min} determines the maximum kinetic energy transferable to the ejected $Si^{(*)}$ recoils, thus the maximum observable Doppler shift. The self-consistency of the binary collision model for the ejection of fast $Si^{(*)}$ atoms is reflected by the fact that a unique value of $R^c_{min}=0.355\pm0.005$ Å has been obtained for all the incidence angles studied. This minimum approach distance corresponds to a threshold value of $E^c_0=4.4$ keV for the incident Ar^+ ions to create an L-shell vacancy in Si and to a minimum transferred kinetic energy of 1.2 keV for the excited Si recoils.

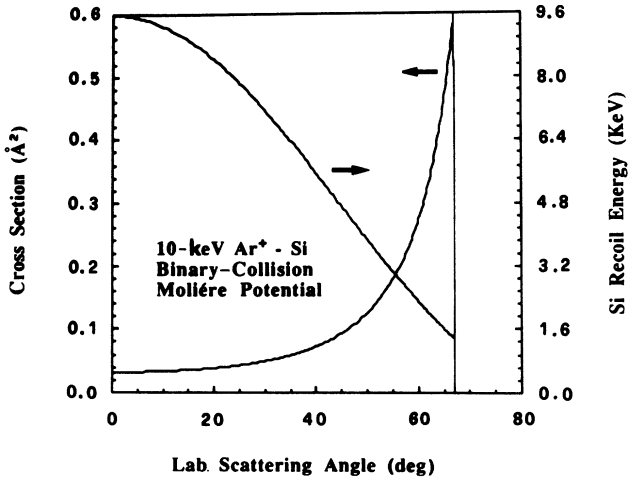

FIG. 8. Calculated Ar-Si inelastic-scattering cross section and transferred energy as a function of laboratory scattering angle using a binary Ar-Si collision model. The Molière approximation to the Thomas-Fermi screening potential has been used. The vertical line corresponds to a critical minimum approach distance of $R^c_{min}=0.355$ Å for Si $2p$ electron excitation, which is determined by the fitting of experimental results.

It is very interesting to note that the value of $R^c_{min}=0.355\pm0.005$ Å in our study is the same as that calculated in a molecular-orbital model by Schneider *et al.*[32] This value is just the sum of the radial distances, d_{med}, corresponding to the maximum electron density of Si $2p$ (0.15 Å) and Ar $2p$ (0.20 Å) orbits.[39] In a recent computer simulation of Ar^+-ion-bombarded Al, Hou *et al.*,[35] using a screened interaction potential, also found a minimum approach distance for Al L-shell excitation which again corresponds to the sum of two d_{med}'s of the $2p$ orbitals. Besides, Pepper's fitting using the fixed sum value of d_{med} yielded good agreement with his Ne^+-Al experimental results.[33] Therefore, this simple sum rule seems to be a good first approximation in calculating the critical approach distance, and thus the threshold energy, for inner-shell vacancy creation in a binary collision, if such excitation is allowed. This consideration would lead us to predict a smaller threshold energy for the Si $2p$ excitation in a Si-Si symmetric collision. This argument would suggest that for low ion incident energies the symmetric collisions should dominate in the inner-shell excitation process while contributions from asymmetric collisions should increase with increasing incident ion energies.

The fitting results for the Doppler shifts for main Auger transition in Si^+ (peak labeled II) are presented in Fig. 7 as continuous lines, where we have used $Q=106.5$ eV (Refs. 13 and 14) and $E_{Auger}-\Phi=74.59$ eV. The best fitting of experimental results is obtained for $R^c_{min}=0.355\pm0.005$ Å. This value is the same as that obtained for the main $Si^{(*)}$ Auger line (peak I), suggesting that the excitation mechanisms are the same for promoting a $2p$ electron to a high-lying ionizing state and for ionizing it.

IV. CONCLUSIONS

In conclusion, we have presented a detailed angle-resolved study for the Si target atomic Auger line shape under 10-keV Ar^+-ion bombardment. The main results can be summarized as follows.

(1) A new atomic Si Auger line at kinetic energy of ~99 eV has been observed for the first time and is tentatively attributed to a transition in Si^+ ions involving two $2p$ holes. We have provided conclusive evidence to support the original suggestion of Thomas *et al.*[14,26] that there exist two atomic Auger peaks situated at 61.36 and 91.1 eV, respectively.

(2) Well-split Doppler peaks have been observed for all

atomic Auger lines; the shift magnitude shows a strong dependence on both incidence and detection angles.

(3) A simple binary Ar-Si asymmetric collision model can successfully account for the observed Doppler shifts, thus for the spatial and energetic distributions of sputtered excited fast moving Si^0 and Si^+ species.

ACKNOWLEDGMENTS

We thank Professor G. Falcone and Professor R. Baragiola for many interesting and stimulating discussions. We are indebted to A. Rotella and M. Bilotti for their collaboration in data analysis. Technical assistance from V. Fabio and E. Li Preti is gratefully acknowledged.

[1] *Sputtering by Particle Bombardment I,* Vol. 47 of *Topics in Applied Physics,* edited by R. Behrisch (Springer-Verlag, New York, 1981); *Sputtering by Particle Bombardment II,* Vol. 52 of *Topics in Applied Physics,* edited by R. Behrisch (Springer-Verlag, New York, 1983).

[2] P. Sigmound, J. Vac. Sci. Technol. A **7**, 585 (1989).

[3] R. A. Baragiola, Radiat. Eff. **61**, 47 (1982).

[4] E. W. Thomas, Vacuum **34**, 1031 (1984).

[5] C. W. White, E. W. Thomas, W. F. Van der Weg, and N. H. Tolk, in *Inelastic Ion-Surface Collisions,* edited by N. H. Tolk (Academic, New York, 1977), Chap. 8.

[6] W. Eckstein, Nucl. Instrum. Methods B **27**, 78 (1987).

[7] K. Saiki and S. Tanaka, Jpn. J. Appl. Phys. **21**, L529 (1982).

[8] A. I. Dodonov, S. D. Fedorovich, E. A. Krylova, E. S. Mashkova, and V. A. Molchanov, Radiat. Eff. **107**, 15 (1988).

[9] F. Xu, R. Siciliano, M. Camarca, and A. Oliva, Surf. Sci. **209**, L133 (1989).

[10] J. Mischler, N. Benazeth, M. Negre, and C. Benazeth, Surf. Sci. **136**, 532 (1984).

[11] J. T. Grant, M. P. Hooker, R. W. Springer, and T. W. Haas, J. Vac. Sci. Technol. **12**, 481 (1975).

[12] K. Wittmaack, Surf. Sci. **85**, 69 (1979).

[13] K. O. Legg, W. A. Metz, and E. W. Thomas, J. Appl. Phys. **51**, 4437 (1980).

[14] R. Whaley and E. W. Thomas, J. Appl. Phys. **56**, 1505 (1984).

[15] C. Benazeth, N. Benazeth, and L. Viel, Surf. Sci. **65**, 165 (1977).

[16] J. J. Vrakking and A. Kroes, Surf. Sci. **84**, 153 (1979).

[17] M. Iwami, S. C. Kim, Y. Kataoka, T. Imura, A. Hitaki, and F. Fujimoto, Jpn. J. Appl. Phys. **19**, 1627 (1980).

[18] R. A. Baragiola, E. V. Alonso, and H. J. L. Raiti, Phys. Rev. A **25**, 1969 (1982).

[19] J. Mischler and N. Benazeth, Scan. Elec. Microsc. **II**, 351 (1984).

[20] G. Zampieri and R. Baragiola, Phys. Rev. B **29**, 1480 (1984).

[21] P. Dahl, M. Robdro, B. Fastrup, and M. E. Rudd, J.Phys. B **19**, 1567 (1976).

[22] A. Bonanno, F. Xu, M. Camarca, R. Siciliano, and A. Oliva, Nucl. Instrum. Methods B (to be published).

[23] Y. Yamauchi, I. Ogoh, R. Shimizu, and H. Hashimoto, Jpn. J. Appl. Phys. **24**, L157 (1985).

[24] U. Fano and W. Lichten, Phys. Rev. Lett. **14**, 627 (1965).

[25] M. Barat and W. Lichten, Phys. Rev. A **6**, 211 (1972).

[26] W. A. Metz, K. O. Legg, and E. W. Thomas, J. Appl. Phys. **51**, 2888 (1980).

[27] K. Saiki and S. Tanaka, Nucl. Instrum. Methods B **2**, 512 (1984).

[28] De Ferraris, O. Grizzi, G. E. Zampieri, E. V. Alonso, and R. A. Baragiola, Surf. Sci. **167**, L175 (1986).

[29] K. Wittmaack, Phys. Lett. **74A**, 197 (1979).

[30] S. Valeri, R. Tonini, and G. Ottaviani, Phys. Rev. B **38**, 13 282 (1988).

[31] T. D. Andreadis, J. Fine, and J. A. D. Matthew, Nucl. Instrum. Methods **209/210**, 495 (1983).

[32] D. Schneider, G. Nolte, U. Wille, and N. Stolterfoht, Phys. Rev. A **28**, 161 (1983).

[33] S. V. Pepper and P. Aron, Surf. Sci. **169**, 14 (1986).

[34] O. Grizzi and R. A. Baragiola, Phys. Rev. A **35**, 135 (1987).

[35] M. Hou, C. Benazeth, and N. Benazeth, Phys. Rev. A **36**, 591 (1987).

[36] S. V. Pepper, Surf. Sci. **169**, 39 (1986).

[37] Chr. Lehmann, *Interaction of Radiation with Solids and Elementary Defect Production* (North-Holland, New York, 1977).

[38] H. H. Andersen, Appl. Phys. **18**, 131 (1979).

[39] J. C. Slater, *Quantum Theory of Matter* (McGraw-Hill, New York, 1968).